CrossMark
← click for updates

Optical detection enhancement in porous volumetric microfluidic capture elements using refractive index matching fluids

M. S. Wiederoder,[a] L. Peterken,[a] A. X. Lu,[b] O. D. Rahmanian,[a] S. R. Raghavan[b] and D. L. DeVoe*[a,b,c]

Porous volumetric capture elements in microfluidic sensors are advantageous compared to planar capture surfaces due to higher reaction site density and decreased diffusion lengths that can reduce detection limits and total assay time. However a mismatch in refractive indices between the capture matrix and fluid within the porous interstices results in scattering of incident, reflected, or emitted light, significantly reducing the signal for optical detection. Here we demonstrate that perfusion of an index-matching fluid within a porous matrix minimizes scattering, thus enhancing optical signal by enabling the entire capture element volume to be probed. Signal enhancement is demonstrated for both fluorescence and absorbance detection, using porous polymer monoliths in a silica capillary and packed beds of glass beads within thermoplastic microchannels, respectively. Fluorescence signal was improved by a factor of 3.5× when measuring emission from a fluorescent compound attached directly to the polymer monolith, and up to 2.6× for a rapid 10 min direct immunoassay. When combining index matching with a silver enhancement step, a detection limit of 0.1 ng mL^{-1} human IgG and a 5 log dynamic range was achieved. The demonstrated technique provides a simple method for enhancing optical sensitivity for a wide range of assays, enabling the full benefits of porous detection elements in miniaturized analytical systems to be realized.

Introduction

Due to its flexibility, low infrastructure requirements, and potential for high sensitivity measurements, optical detection is a preferred sensing modality for many point-of-care diagnostic assays.[1] Interactions between incident photons and target analytes may be probed using a wide variety of optical sensing mechanisms including absorbance, colorimetric, fluorescence, interferometric, or spectroscopic detection. Optical detection is nearly ubiquitous for rapid point-of-care molecular diagnostic tests, an area that is presently dominated by lateral flow assays.[2,3] In these tests, sample migrating through a porous substrate by capillary action binds with colored or fluorescent antibody-functionalized microparticles. Downstream capture of these antigen-specific particles by secondary probes results in selective particle accumulation, allowing qualitative analysis

by direct optical observation, or semi-quantitative readout using a calibrated colorimetric or fluorescence reader. To improve on the performance of lateral flow tests, microfluidic technology has been widely explored for the development of next-generation point-of-care assays.[3] By taking advantage of various functionalization routes to anchor proteins, peptides, nucleic acids, or other assay-specific capture probes to the internal surfaces of microchannels, microfluidic technology offers great potential to realize improved assay throughput, reduce sample requirements, and enhance multiplexing capabilities. The surface-to-volume ratio scales favourably in microfluidic systems, such that smaller channels reduce the total sample volume required to deliver a fixed number of target molecules to capture probes anchored on the channel surface. However, the use of planar capture surfaces imposes a basic limitation on assay performance, since each channel wall may be functionalized with, at most, a single monolayer of probes. As a result, assay sensitivity and dynamic range are both constrained by the geometry of the capture surface.

As an alternative to planar capture surfaces, porous flow-through capture zones have been explored as an approach to realizing volumetric detection elements in microfluidic systems, allowing reaction site density to be greatly

[a] *Department of Bioengineering, University of Maryland, College Park, Maryland, USA*

[b] *Department of Chemical and Biomolecular Engineering, University of Maryland, College Park, Maryland, USA*

[c] *Department of Mechanical Engineering, University of Maryland, College Park, Maryland, USA. E-mail: ddev@umd.edu; Tel: +1 301-405-8125*

enhanced.[4,5] By minimizing pore dimensions for a given application, this approach offers the further benefit of reducing the characteristic diffusive length scales associated with interactions between target molecules in solution and molecular probes attached to the porous matrix surface, thereby enhancing assay speed. For optical detection, however, light scattering by micrometre-scale pores within a volumetric capture matrix presents an inherent constraint that can severely degrade sensor performance. Variations in the dielectric constant between the porous matrix and fluid within the open pores result in strong coupling with incident light of wavelengths on the same order as the characteristic pore dimensions, leading to scattering of photons passing through the matrix.[6] Light scattering due to multiple changes in refractive index (n) significantly decreases optical transparency, with a concomitant reduction in sensitivity for measurements based on optical absorbance of target molecules or complexes within the detection zone. For fluorescence assays, transmission of photons associated with fluorophore excitation and emission can be reduced, similarly constraining measurement sensitivity. In general, regardless of the optical detection method, higher scattering results in a reduction of the probed volume, and thus a reduction in assay sensitivity.

Here we demonstrate the use of index-matching fluids to enhance optical performance in porous microfluidic capture elements. By infusing a fluid with the same refractive index as the porous medium itself, optical gradients within the detection volume may be reduced or eliminated, thereby minimizing light scattering and facilitating true volumetric detection within the functionalized porous sensor element. Fluorescence signal enhancement is demonstrated using porous polymer monoliths, with proof of concept shown by enhancing fluorescence signal of glutaraldehyde attached to the monolith, and biomolecular detection demonstrated through a direct fluorescence immunoassay with up to 2.6× signal amplification. Application of the index-matching technique is further demonstrated for an absorbance-based immunoassay with silver enhancement of gold nanoparticle (AuNP) labelled IgG, using a silica bead packed bed with an ordered porous structure in a thermoplastic microfluidic chip. For the absorbance based direct assay, a detection limit of 0.1 ng mL^{-1} was achieved, with linear dynamic range of at least 5 logs, and up to two orders of magnitude higher sensitivity than related thermoplastic planar microfluidic immunosensors.[7]

Methods and materials

Materials

Glycidal methacrylate (GMA), hydrochloric acid (HCl), cyclohexanol, sodium hydrosulfide, citric acid, sodium citrate, sulphuric acid, 2,2-dimethoxy-2-Phenylacetophenone (DMPA), sodium phosphate dibasic, phosphate buffer saline (PBS), fluorescein isothiocyanate (FITC) labelled rabbit IgG, glutaraldehyde, bovine serum albumin (BSA), human IgG, (3-aminopropyl) triethoxysilane (APTES), cyclohexane, sucrose, tris

buffer, and hydroquinone were purchased from Sigma-Aldrich (St. Louis, MO). Ethoxylated trimethylolpropane triacrylate (SR454) is purchased from Sartomer (Warrington, PA). Bis-(sulfosuccinimidyl) suberate (BS3), goat anti-rabbit IgG, and N-(γ-maleimidobutyryloxy) sulfosuccinimidyl ester (GMBS) were purchased from Thermo Fisher Scientific Inc. (Rockford, IL). Silver enhancement solution and 5 nm gold nanoparticle tagged anti-human IgG were purchased from Cytodiagnostics (Burlington, ON). Silica beads (20 μm diameter) were purchased from Corpuscular, Inc. (Cold Spring, NY). Silver acetate was purchased from Carolina Biological Supply Co. (Burlington, NC). Microfluidic fittings were purchased from IDEX Health & Science (Oak Harbor, WA) and needle tubing was purchased from Hamilton Syringe (Reno, NV). Capillary tubing with 360 μm O.D. and 250 μm I.D. was purchased from Polymicro Technologies (Phoenix, AZ).

Capillary monolith immunoassay with fluorescence readout

GMA monoliths were formed in a silica capillary using a previously developed procedure.[4] After conditioning the capillary with 0.1 M HCl, a pre-monolith solution consisting of GMA (16% w/w), ethoxylated trimethylolpropane triacrylate (SR454) (24% w/w), cyclohexanol (50% w/w), methanol (10% w/w) was created. Next the photoinitiator 2,2-dimethoxy-2-phenylacetophenone (DMPA) was added at a ratio of 1 : 100 w/w with respect to the combined weight of the GMA and SR454. The combined solution was infused into the capillary masked with aluminium foil, and exposed to UV light with an incident power of 22.0 mW cm^{-2} for 10 min. After UV-exposure the monolith section was rinsed with methanol and 20% methanol (v/v) aqueous solution and incubated with 2 M sodium hydrosulfide in a methanol–0.1 M aqueous sodium phosphate dibasic (20 : 80, v/v) for 2 h to transform epoxide groups to thiol groups. Remaining epoxide groups were hydrolysed by overnight incubation at 65 °C with 0.5 M sulphuric acid before rinsing with deionized water and ethanol. Finally 2 mM GMBS in ethanol was infused for 1 h followed by PBS rinsing to create amine-reactive NHS ester groups.

Initial fluorescence enhancement was demonstrated by infusing aqueous solutions of glutaraldehyde, an autofluorescent organic compound, through the monolith for direct attachment to the reactive monolith surface. This was followed by rinsing with deionized water for 5 min at 1 μL min^{-1} and infusion of GMA monomer for 5 min at 1 μL min^{-1} for refractive index matching. Next a direct assay was completed with the experimental setup shown in Fig. 1.

First 50 μg mL^{-1} goat anti-rabbit IgG in phosphate buffered saline (PBS) was infused for 1 h matching at 1 μL min^{-1} to react primary amines with exposed NHS ester groups on the GMBS treated monolith surface, followed by infusion of 2 mg mL^{-1} bovine serum albumin (BSA) in PBS matching at 1 μL min^{-1} for 15 min to block remaining reactive sites. This was followed by infusion of fluorescein isothiocyanate (FITC) labelled rabbit IgG at 2 μL min^{-1} for 5 min at concentrations of either 0.1, 1.0, or 10 g mL^{-1}. In each case, 2 mg mL^{-1} BSA in PBS was included with the immunoglobulins to serve as a
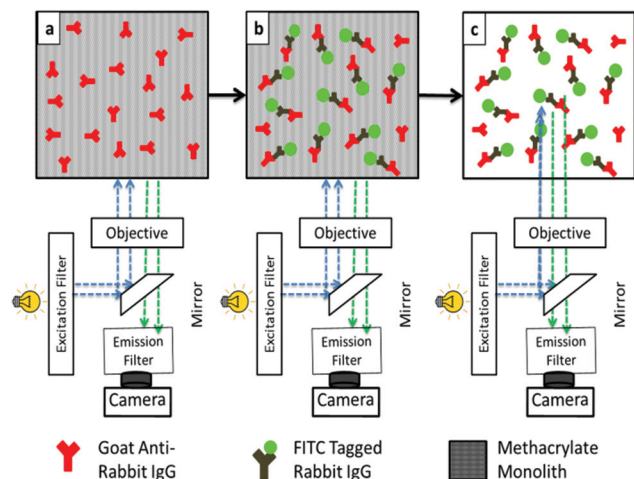
Fig. 1 Experimental process for fluorescence based direct assay. The methacrylate monolith is covalently functionalized with goat anti-rabbit IgG (a) followed by infusion of FITC tagged rabbit IgG resulting in immobilization (b). Next GMA ($n = 1.45$) was infused to enhance the fluorescence signal (c).

dynamic blocking agent. Following IgG introduction, the monolith was rinsed with deionized water for 5 min at 1 μL min^{-1}, and GMA monomer was infused through the monolith for 5 min at 1 μL min^{-1} for index matching. Imaging was performed using a B-2E/C filter cube (465–495 nm excitation, 515–555 nm emission) equipped on a TE-2000-S inverted epi-fluorescence microscope (Nikon, Melville, NY) with a CoolSnap HQ2 8-bit CCD camera (Roper Scientific, Tucson, AZ). An excitation wavelength within the range of 465–495 nm was selected using a B-2E/C blue filter (Nikon). Images were acquired continuously during water infusion and index-matching solution infusion. A region of interest 500 μm after the monolith beginning approximately 1 mm long and 150 μm tall was selected over the monolith section for before and after analysis using NIS elements software (Nikon).

Microfluidic packed silica bead immunoassay with absorbance readout

Thermoplastic plates for fabrication were made with Zeonor 1020R cyclic olefin polymer (COP) resin (Zeon Chemicals, Louisville, KY) using a hot press (AutoFour/15, Carver, Inc., Wabash, IN). COP chips were cut to the desired size before channels and fluidic access ports were milled with a 3-axis desktop CNC milling machine (MDX-650, Roland DGA, Irvine, CA) and sonicated to remove debris. Channels were 150 μm deep and 300 μm wide in the sensing region with 40 μm deep and 50 μm wide regions which served as weirs to facilitate bead packing. The milled side and unmilled mating side were washed with methanol, isopropanol, and deionized water before N$_2$ drying and overnight degassing at 75 °C. The device was then solvent bonded with cyclohexane using an established procedure.[8,9] Briefly the channel side was exposed to

cyclohexane at 30 °C for 7.5 min before manual alignment and pressing with the mating side. The multilayer chip was then pressed at 1.38 MPa for 1 min at room temperature to complete the bonding.

Silica beads in a 5 wt% aqueous solution were functionalized with amine groups based on a previously reported method.[10] The beads were washed in piranha solution for 1 h before rinsing three times with deionized water and ethanol. Amine groups were introduced by incubating the beads in a solution of 5% (3-aminopropyl) triethoxysilane (APTES), 5% deionized water, and 90% ethanol (v/v) under agitation for 1 h at room temperature and washed 3 times with ethanol and PBS. Human IgG was attached to the beads using BS3, a homo-bifunctional amine-reactive crosslinker, by combining 900 μL of human IgG serially diluted in PBS, 100 μL of bead solution, and 35 μL of 7.19 mM BS3 in deionized water and incubating 30 min under agitation at room temperature. Control beads were functionalized by substituting human IgG with 2 mg mL^{-1} BSA in PBS. The reaction was quenched by adding 100 μL of 1 M tris buffer before agitating for 15 min at room temperature. The resulting mixture was washed 3 times with PBS and suspended in 2 mg mL^{-1} BSA in PBS overnight at 4 °C.

Functionalized beads were packed into a microfluidic device using vacuum through the side access channel into the restricted sensing region using a syringe and needle in the fluidic outlet port. Fluidic interfaces for off chip syringe pumps were created by inserting needle tubing segments into the access ports following a previously reported method[11] after the packed bed was formed. Fluidic fittings were attached to the needles and tests were conducted immediately.

Silver enhancement

To prepare a device for silver enhancement, 2 mg mL^{-1} BSA in PBS was infused for 15 min at 2 μL min^{-1} to prevent non-specific protein binding. Next, a splitter valve attached to the side channel was closed to ensure flow through the packed bed. Gold nanoparticle (AuNP) anti-human IgG conjugate solution was diluted 1 : 50 in 2 mg mL^{-1} BSA in PBS and infused for 15 min at 2 μL min^{-1} followed by rinsing with 2 mg mL^{-1} BSA in PBS for 10 min at 2 μL min^{-1}. Silver enhancement solution was prepared using a two part mixture[12] chosen due to its stability under light exposure, consisting of 0.5 mg silver acetate in 5 mL deionized water and 1.25 mg hydroquinone in citrate buffer at pH 3.8. Deionized water was infused for 5 min followed by a 5 min infusion with silver enhancement solution combined in an off chip junction and a 5 min rinse with deionized water at 2 μL min^{-1} for each solution. Finally an aqueous index matching solution of 68% sucrose (w/w) was infused for 5 min at 3 μL min^{-1}. The experimental setup is shown in Fig. 2.

Images of the chip before and after silver enhancement and after sucrose infusion were captured using an AZ 100 Multi-zoom microscope (Nikon) with diascopic lighting (see Fig. 2). Illumination was provided by a halogen lamp without filtering. Images were analysed using NIS elements software. The region
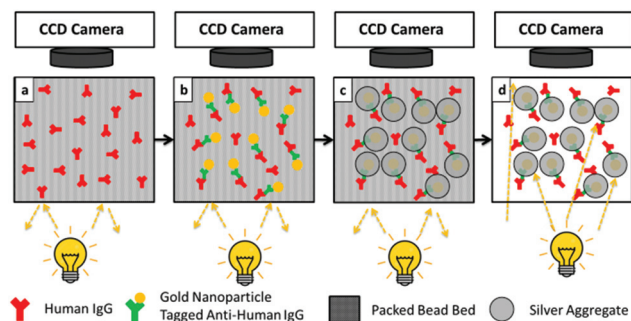
Fig. 2 Experimental process for direct immunoassay using transmittance based detection. (a) A packed bed of silica beads with human IgG is (b) infused with anti-human IgG attached to gold nanoparticles (AuNP) that are (c) silver enhanced to create large aggregates prior to (d) introduction of index matching sucrose solution to render the volumetric matrix transparent for optical absorbance measurements.

Fig. 3 (a) An opaque monolith sheet in air ($n \sim 1$) remains semi-opaque due to light scattering when water ($n \sim 1.33$) is introduced. The addition of index-matching aqueous sucrose ($n \sim 1.46$) significantly enhances transparency, revealing the image beneath. (b) Fluorescent intensity (I, arbitrary units) following water ($I = 758$) and GMA monomer ($I = 2644$) infusion through a glutaraldehyde functionalized monolith in a glass capillary.

of interest (ROI) used to determine the intensity of the packed bed was taken from the middle third with respect to the x and y dimensions. In instances where bubbles were observed to form during sucrose infusion, regions containing bubbles were omitted from analysis. Transmittance (T) was determined as the average light intensity of the ROI divided by the intensity of a nearby featureless area, and the absorbance (A) was defined as $1 - T$.

Results and discussion

Fluorescence detection in porous GMA monoliths

Selection of an appropriate index-matching fluid for microfluidic assays requires consideration of multiple factors such as optical clarity, viscosity, material compatibility, price, safety, and biocompatibility. For example, many commercially available organic solvents or oils with suitable refractive indices matched to the porous matrices explored in this work are either too viscous for infusion, not biocompatible, or incompatible with microfluidic device materials such as thermoplastics. Some aqueous index-matching solutions are compatible with thermoplastics and offer lower viscosity, but contain high salt concentrations that reduce antibody binding affinity and remove the target biomarker from the capture matrix. Alternate index-matching solutions are necessary for the technique to be useful for practical microfluidic assays.

The utility of index matching within a monolith structure to enhance optical transparency is shown by Fig. 3a. The monolith is approximately 1 mm thick and the picture beneath is 2 mm in diameter. The monolith was photographed in air ($n = 1$), after adding water ($n = 1.33$), and after adding 68% aqueous sucrose solution w/w ($n = 1.46$). As the refractive index of the solution approaches that of the monolith structure, light scattering within the monolith volume is reduced, facilitating visualization of the underlying image as the monolith transparency increases.
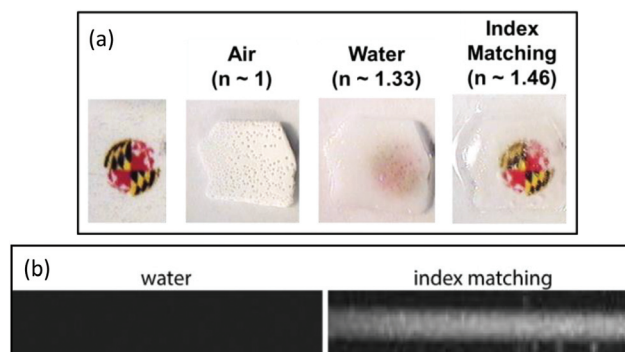
In the case of fluorescence detection, the porous medium used to support volumetric detection in this work consists of a GMA monolith anchored to the walls of a glass capillary. While detection of fluorescent species immobilized to the surface of silica capillaries[13–15] has been demonstrated, the use of a polymer monolith as a porous supporting scaffold can serve to increase volumetric probe density and reduce diffusion length scale significantly compared with the use of open capillary systems. The monolith structure is a cylinder 250 μm in diameter and 1–2 mm long composed of spherical microglobules approximately 1 μm in diameter with an average pore size of 3–5 μm that create a tortuous flow path with high surface area for capturing probe immobilization.[4] Here we explored the use of GMA monomer ($n = 1.45$) as a refractive-index-matching fluid. The monomer possesses a low viscosity similar to that of water, with a refractive index well matched with that of the monolith structure itself. Prior to introduction into the monolith, the GMA monomer was filtered to remove particles larger than 200 nm, but no additional chemical purification of the product was performed. Despite the relatively reactive nature of GMA, under the lighting conditions used in this work no observable polymerization was evident for GMA monomer in the absence of photoinitiator and crosslinker. We note that because GMA exhibits moderate toxicity, proper care should be taken during operation and disposal of devices employing this monomer for index matching. The GMA monomer was also found to result in some degree of quenching of the native autofluorescence of the monolith. Compared to the nominal fluorescence intensity measured for a non-functionalized monolith in air, the same monolith placed in water exhibited a 26% reduction in autofluorescence. In contrast, when placing the monolith in GMA a 48% reduction in fluorescence intensity was observed. To evaluate the impact of GMA index matching on the emitted optical signal for a fluorescent species, glutaraldehyde was immobilized through
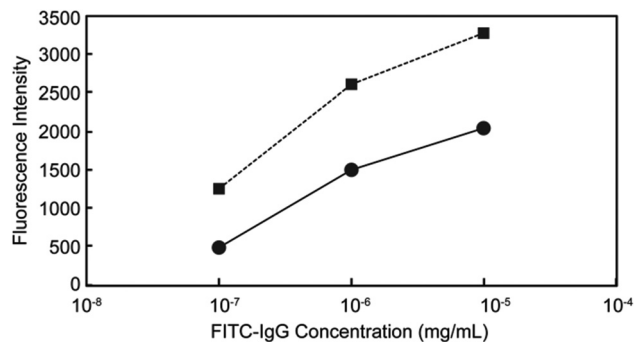
Fig. 4 Direct assay with fluorescein isothiocyanate labelled antibodies before and after infusion of GMA monomer through GMA-based monolith capture element in a glass capillary.

direct covalent bonding to amine groups on the monolith surface. Compared to the case of water, the fluorescence intensity of a glutaraldehyde functionalized monolith perfused with GMA monomer was found to increase by a factor of 3.5×, as seen in Fig. 3b.

To investigate the use of GMA monomer as an index-matching fluid for assays involving biomolecules, a direct immunoassay using FITC-tagged rabbit IgG was explored. A polymer monolith within a silica capillary was functionalized with goat anti-rabbit IgG before infusion with 0.1, 1.0, and 10 ng mL^{-1} of FITC-tagged IgG in PBS. The fluorescence intensity during water infusion and during GMA infusion is shown in Fig. 4. As evident from this figure, index matching with the GMA monomer solution significantly enhances the fluorescence signal, with increasing amplification as the analyte concentration is reduced. A maximum signal enhancement factor of 2.6× was observed at the lowest concentration of 0.1 ng mL^{-1} evaluated in this experiment. It is also notable that the assay was completed within 10 min of sample introduction, reflecting the ability of the porous matrix to encourage rapid probe–analyte interactions.

Absorbance detection in packed silica bead beds

Packed beds of microbeads are commonly used in both capillary and microfluidic systems as solid phase extraction media, stationary phases for chromatographic separations, and high area reactive surfaces. When combined with index matching, the use of packed beds as volumetric biodetection elements offers several advantages over *in situ* photopolymerized monoliths. Fabrication of a microfluidic packed bed is relatively straightforward, requiring only a simple weir structure to prepare the bed. Beads manufactured from a wide variety of materials with tailored sizes are readily available, allowing precise selection of bulk and surface properties as well as pore dimensions. Furthermore, conjugation of capture probes to the bead surface may be performed off-chip prior to bed packing, greatly simplifying the overall biosensor preparation process and providing a facile route to multiplexing.

Here we investigate the use of silica beads to prepare packed sensor beds in thermoplastic microfluidic chips, with

aqueous sucrose solutions used as an inexpensive, low-viscosity, and biocompatible index-matching fluid. The refractive index of aqueous sucrose solutions varies nearly linearly with sucrose concentration, over a range of 1.33 for pure water to 1.50 for an 84% sucrose solution by weight.[16] Silica exhibits a refractive index of 1.46,[17] which is well matched by a sucrose concentration of 68%. To validate this assumption, the optimal index-matching solution was determined by infusing prepared aqueous sucrose solutions of various weight percentages through a packed bed of 20 μm diameter silica beads while measuring transmittance of light through the bed. As shown in Fig. 5, a maximum transmittance of 96.8% was observed during infusion of 68% sucrose solution, as anticipated. In addition the transmittance magnitude is relatively insensitive for aqueous sucrose concentrations between 56% ($n \sim 1.43$) to 74% ($n \sim 1.48$). Sucrose concentrations greater than 74% were found to be too viscous for reliable perfusion through the porous silica bead beds.

Because direct observation of absorbance changes resulting from the accumulation of native target biomolecules results in high detection limits, some form of optical enhancement is typically employed for absorbance-based assay readout, for example through the application of enzymatic amplification or use of a secondary probe capable of generating a high absorbance signal. Here we combine index matching in a packed microfluidic silica bead bed with the latter method, together with a silver amplification step to further increase assay sensitivity. Silver amplification was chosen due to the ease of handling, inexpensive reagents, robustness, and high sensitivity.[18] In this method, micrometre-scale silver clusters are grown on AuNP labelled biomolecular probes, resulting in large absor-
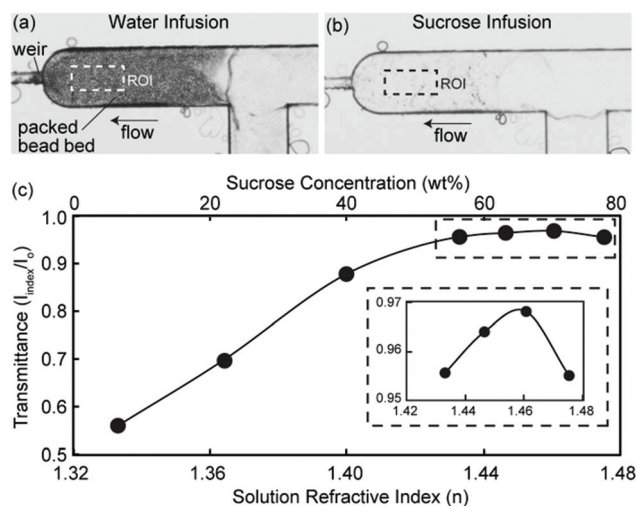

Fig. 5 Images of a packed silica bead bed infused with (a) water and (b) 68% sucrose in water ($n = 1.46$). (c) Measured light transmittance with varying sucrose concentration. Transmittance is defined as the ratio of average transmitted intensity of a region of interest (ROI) of the packed bed after sucrose infusion (I_{index}) to the background intensity (I_o) of a nearby region of the chip.

bance signals for the resulting assay. This approach has been previously demonstrated for enhanced optical detection of many biological targets including nucleic acids[19,20] as well as antibodies[21–24] and other proteins[25,26] with detection relying on colorimetric readers,[20] scanometric methods,[19,22,26] CCD cameras,[23,24] or direct visual inspection[27] with the naked eye to detect silver aggregate formation.[18] However, many optical immunoassays employing silver enhancement are presently limited in their utility for near-patient use. Existing assays use planar capture surfaces that limit the number of biomarker recognition events and detector sensitivity. To overcome this limitation long incubation times and repeated hand pipetting are required that are not conducive to rapid diagnostics. Many studies use glass and silicon based devices that can be fragile and are often too expensive for disposable near-patient tests, or silicone elastomers that are not economically viable for high throughput production.[28–31] For thermoplastic substrates, challenging immobilization chemistries limit the capture probe density and thus assay sensitivity.[7,21] Thus we propose combining off chip functionalized elements into a low-cost thermoplastic device that is adaptable to large-scale manufacturing.

The combination of index matching and silver amplification in a volumetric silica bead bed was investigated using a thermoplastic COP chip design. The fabricated chip contains a contains a weir for trapping silica beads injected through a side port to create a packed bed with a nominal pore size of ~5 μm, together with an inlet port for the introduction of AuNP-labelled sample, silver amplification solutions, and index-matching fluid (Fig. 6a). Using this platform, a dilution study was performed to evaluate the impact of index matching on assay sensitivity and dynamic range. The bead bed is initially white before infusion of AuNP anti-human IgG conjugates. Beads conjugated with relatively high human IgG concentrations (>10 μg mL^{-1}) will become pink to the naked eye after AuNP conjugate binding while those with less human IgG will remain white even though AuNP conjugates are captured. Following introduction of silver enhancement solution the white bead bed begins to darken to a reddish-brown as silver aggregates form on the captured AuNP's. No removal of silver aggregates due to shear forces generated by the relatively high viscosity of the aqueous sucrose solution was observed at the flow rates used. As seen in Fig. 6a, increasing concentration of immobilized human IgG leads to the formation of more silver aggregates in the bead bed that absorb the incident light.

Example images of the porous detection matrix following silver amplification and index matching are shown in Fig. 6b for two representative concentrations of human IgG bound to the beads. The relative absorbance, defined as the ratio of absorbance after index matching (A_{index}) to the absorbance after silver enhancement and water rinsing but before index matching (A_o), was analysed to evaluate detection limit, dynamic range, and sensitivity. By employing relative absorbance as the assay output, the impact of variations in lighting conditions caused by fluctuations in ambient lighting and
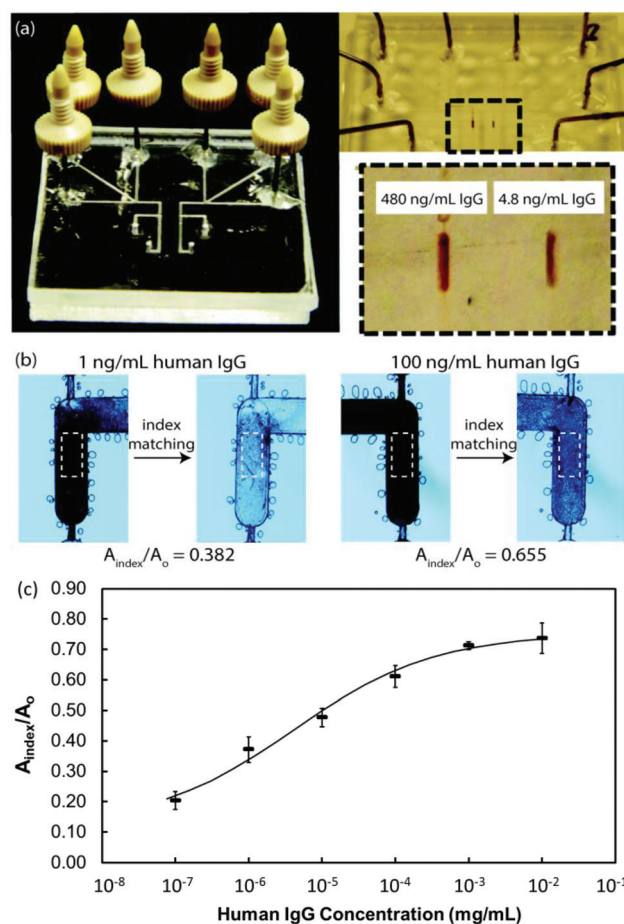

Fig. 6 (a) Microfluidic chip containing silica bead detection zones, with the bead beds alternately functionalized with either 480 ng mL^{-1} or 4.8 ng mL^{-1} of human IgG. The magnified image of the packed bed is shown after selective capture of AuNP anti-human IgG conjugates and subsequent silver amplification. (b) Absorbance was measured for the regions of interest shown (dashed boxes) after silver enhancement and water rinse, and after infusion with a 68% sucrose solution for index matching. (c) Relative absorbance for a silver-enhanced direct immunoassay following infusion of index matching solution in a microfluidic silica bead bed.

lamp output, as well as variations in chip geometry that might impact optical performance, were minimized to reduce signal variance across test devices.

Relative absorbance measurements from a dilution study covering a range of human IgG concentration from 0.1 ng mL^{-1} to 10 μg mL^{-1} are presented in Fig. 6c. From inspection of this data, and defining a conservative noise floor as the average relative absorbance of the negative control monolith plus 3 standard deviations (0.189), a minimum detectable signal of 0.1 ng mL^{-1} (0.65 pM) was achieved. For comparison, the minimum detectable human IgG concentration before and after silver enhancement with water infusion was 10 μg mL^{-1}, revealing the significant benefits of index matching to assay sensitivity. At high analyte concentrations, signal saturation is observed above 1 μg mL^{-1} (student's t test with $p < 0.05$) thus

defining an overall dynamic range of 5 logs (0.1 ng mL^{-1} to 1 µg mL^{-1}). Each dilution tested within this range is well differentiated from each other ($p < 0.05$) demonstrating good control of signal noise. The data is consistent with a sigmoidal dependence between optical signal and antibody concentration, as expected based on Langmuir binding kinetics.[32,33] Compared with microfluidic immunoassays requiring significantly longer assay times on the order of 60–90 min,[7,34] the demonstrated molar detection limit is approximately 1–2 logs lower than these previously reported devices employing planar capture surfaces. The improved sensitivity and large dynamic range confirm the utility of index matching as a strategy for enhancing the performance of optical detection from three dimensional porous matrices. Furthermore, we note that for the particular device implementation explored in this work, the low material and fabrication costs associated with thermoplastic microfluidics offers potential for disposable diagnostics that may be used at the point of care, while the robustness of the optical detection scheme supports integration with a portable photodetector or camera, LED excitation source, and lightweight power supply for use in remote and resource-limited environments.

Several potential practical limitations of the technique should be noted. For any particular application, issues relating to the viscosity and biocompatibility of candidate index matching fluids must be carefully considered, and for the case of sensors involving biomolecular interactions, the potential degradation of these interactions by the index matching fluid must also be evaluated. The addition of index matching as a required step increases assay complexity, while the integration of porous microfluidic capture elements can present its own challenges compared to simpler planar surface modification methods. Regardless, the significant improvement in assay performance that can be achieved using the reported method, in terms of both assay sensitivity and time, offers a promising solution for a wide variety of demanding microfluidic sensing applications.

Conclusions

This work demonstrates refractive index matching as a flexible method for enhancing optical signals in microfluidic assays with porous volumetric detection elements. The technique facilitates the advantages of porous sensing elements such as rapid assay times and sensitive volumetric analyte capture while minimizing the effects of light scattering that compromise optical measurement sensitivity. Fluorescent signal was amplified by a factor of 3.5× for attached fluorescent glutaraldehyde and 2.6–1.6× for a direct immunoassay that took ~10 min to complete. For an absorbance-based direct assay using silver enhancement, the detection limit was 0.1 ng mL^{-1} with a 5-log dynamic range and a total time of 45 min to complete. These results demonstrate volumetric optical detection techniques that could be adapted for detection of numerous biomarkers such as bacteria, viruses, proteins, toxins, or nucleic acids. Future development applied to simple, low cost point-of-care devices for environmental monitoring or medical diagnostic tests can improve detection limits, allow quantification of dilute targets, and reduce total assay times compared to existing technology.

Acknowledgements

Notes and references

1 American Academy of Microbiology, *Bringing the Lab to the Patient: Developing Point-of-Care Diagnostics for Resource Limited Settings*, 2011.

2 C. D. Chin, V. Linder and S. K. Sia, *Lab Chip*, 2012, **12**, 2118–2134.

3 P. Yager, G. J. Domingo and J. Gerdes, *Annu. Rev. Biomed. Eng.*, 2008, **10**, 107–144.

4 J. Liu, C.-F. Chen, C.-W. Chang and D. L. DeVoe, *Biosens. Bioelectron.*, 2010, **26**, 182–188.

5 A. K. Ellerbee, S. T. Phillips, A. C. Siegel, K. a Mirica, A. W. Martinez, P. Striehl, N. Jain, M. Prentiss and G. M. Whitesides, *Anal. Chem.*, 2009, **81**, 8447–8452.

6 J. M. S. Saarela, S. M. Heikkinen, T. E. J. Fabritius, a T. Haapala and R. a Myllylä, *Meas. Sci. Technol.*, 2008, **19**, 055710.

7 J. Wen, X. Shi, Y. He, J. Zhou and Y. Li, *Anal. Bioanal. Chem.*, 2012, **404**, 1935–1944.

8 C.-F. Chen, J. Liu, C.-C. Chang and D. L. DeVoe, *Lab Chip*, 2009, **9**, 3511–3516.

9 O. Rahmanian, C.-F. Chen and D. L. DeVoe, *Langmuir*, 2012, **28**, 12923–12929.

10 Z.-H. Wang and G. Jin, *J. Immunol. Methods*, 2004, **285**, 237–243.

11 C. F. Chen, J. Liu, L. P. Hromada, C. W. Tsao, C. C. Chang and D. L. DeVoe, *Lab Chip*, 2009, **9**, 50–55.

12 G. W. Hacker, L. Grimelius, G. Danscher, G. Bernatzky, W. Mussl, H. Adam and J. Thurner, *J. Histotechnol.*, 1988, **11**, 213–221.

13 U. Narang, P. R. Gauger, a W. Kusterbeck and F. S. Ligler, *Anal. Biochem.*, 1998, **255**, 13–19.

14 C. Mastichiadis, S. E. Kakabakos, I. Christofidis, M. a. Koupparis, C. Willetts and K. Misiakos, *Anal. Chem.*, 2002, **74**, 6064–6072.

15 S. Lane, P. West, A. François and A. Meldrum, *Opt. Express*, 2015, **23**, 7994–8006.

16 International Commission for Uniform Methods of Sugar Analysis, 1974.

17 R. Budwig, *Exp. Fluids*, 1994, **17**, 350–355.

18 R. Liu, Y. Zhang, S. Zhang, W. Qiu and Y. Gao, *Appl. Spectrosc. Rev.*, 2014, **49**, 121–138.

19 T. A. Taton, C. A. Mirkin and R. L. Letsinger, *Science*, 2000, **289**, 1757–1760.

20 W.-J. Yang, X.-B. Li, Y.-Y. Li, L.-F. Zhao, W.-L. He, Y.-Q. Gao, Y.-J. Wan, W. Xia, T. Chen, H. Zheng, M. Li and S.-Q. Xu, *Anal. Biochem.*, 2008, **376**, 183–188.

21 C. D. Chin, T. Laksanasopin, Y. K. Cheung, D. Steinmiller, V. Linder, H. Parsa, J. Wang, H. Moore, R. Rouse, G. Umviligihozo, E. Karita, L. Mwambarangwe, S. L. Braunstein, J. van de Wijgert, R. Sahabo, J. E. Justman, W. El-Sadr and S. K. Sia, *Nat. Med.*, 2011, **17**, 1015–1019.

22 C.-H. Yeh, C.-Y. Hung, T. C. Chang, H.-P. Lin and Y.-C. Lin, *Microfluid. Nanofluid.*, 2008, **6**, 85–91.

23 R.-Q. Liang, C.-Y. Tan and K.-C. Ruan, *J. Immunol. Methods*, 2004, **285**, 157–163.

24 M. Yang and C. Wang, *Anal. Biochem.*, 2009, **385**, 128–131.

25 Y. Wang, D. Li, W. Ren, Z. Liu, S. Dong and E. Wang, *Chem. Commun.*, 2008, 2520–2522.

26 L. Ding, R. Qian, Y. Xue, W. Cheng and H. Ju, *Anal. Chem.*, 2010, **82**, 5804–5809.

27 C. D. Chin, T. Laksanasopin, Y. K. Cheung, D. Steinmiller, V. Linder, H. Parsa, J. Wang, H. Moore, R. Rouse, G. Umviligihozo, E. Karita, L. Mwambarangwe, S. L. Braunstein, J. van de Wijgert, R. Sahabo, J. E. Justman, W. El-Sadr and S. K. Sia, *Nat. Med.*, 2011, **17**, 1015–1019.

28 D. Desai, G. Wu and M. H. Zaman, *Lab Chip*, 2011, **11**, 194–211.

29 M. Geissler, E. Roy, G. a. Diaz-Quijada, J.-C. Galas and T. Veres, *ACS Appl. Mater. Interfaces*, 2009, **1**, 1387–1395.

30 H. Sharma, D. Nguyen, A. Chen, V. Lew and M. Khine, *Ann. Biomed. Eng.*, 2011, **39**, 1313–1327.

31 P. Yager, T. Edwards, E. Fu, K. Helton, K. Nelson, M. R. Tam and B. H. Weigl, *Nature*, 2006, **442**, 412–418.

32 B. Kurtinaitiene, D. Ambrozaite, V. Laurinavicius, A. Ramanaviciene and A. Ramanavicius, *Biosens. Bioelectron.*, 2008, **23**, 1547–1554.

33 V. C. Rucker, K. L. Havenstrite and A. E. Herr, *Anal. Biochem.*, 2005, **339**, 262–270.

34 K. F. Lei and K. S. Wong, *Instrum. Sci. Technol.*, 2010, **38**, 295–304.